CHAPTER 2

CFD STUDY OF TISSUE ENGINEERING SCAFFOLD

Mohamad Shukri Zakaria[1], Muhammad Luqman Ghazali[1], Kahar Osman[2], Nur Hazwani Mokhtar[1], S. K. Badreddin Giuma[2], Mizah Rami[1], Nofrizalidris Darlis[3]*

[1]Fakulti Teknologi Kejuruteraan Mekanikal, Universiti Teknikal Melaka, Hang Tuah Jaya 76100, Durian Tunggal, Melaka

[2]Fakulti Kejuruteraan Mekanikal, Universiti Teknologi Malaysia, Skudai, Johor

[4] Centre of Automotive & Powertrain Technology, Faculty of Engineering Technology, Universiti Tun Hussein Onn Malaysia, Edu Hub Pagoh, 84600, Muar, Johor, Malaysia

2.0 INTRODUCTION

In the tissue engineering field, bone tissue engineering (BTE) is regarded as a potential strategy for the development and growth of new bone tissues. To promote cell growth and the transfer of nutrients, bone scaffolds should have an interconnected pore structure and mechanical characteristics close to those of the surrounding tissues [1]. The goal of tissue engineering is to create innovative biofunctional tissues as well as to rejuvenate and heal diseased or damaged tissue. In 2017, there were over 22.3 million orthopedic surgical procedures conducted globally; by 2022, that number is expected to surpass 28.3 million [2].

Porous three-dimensional structures known as scaffolds are composed of materials with appropriate qualities like biocompatibility, mechanical strength, biodegradability, and osteoconductive ability [3]. The high surface areas, adsorption capacities, and catalytic qualities of porous solids are widely acknowledged. In to achieve optimal performance of bone scaffolds, various type of nature scaffolds have been designed and reported, such as spider-web, sunflower, honeycomb, nautilus shell and giant water lily. The bioinspired tracheal scaffold exhibited excellent performance and was able to customize itself with the help of 3D printing, considering the different sizes of the trachea.

Permeability and wall shear stress (WSS) are important biological properties because of their role in cellular activity inside scaffolds [4]. Research on how fluid flow behavior affects the degradation of polymetric scaffolds with varying porosity and permeability has revealed that, because of their higher initial stiffness, lower porosity and permeability values resulted in higher rates of degradation and shorter scaffold lives [5]. Consequently, estimating and forecasting the shear stress that fluid flow will cause on a scaffold's walls can be a useful first step in managing perfusion in cell culture procedures [4].

Permeability refers to the ability of liquids, gases, or specific chemicals to pass through a material. It is typically measured by assessing the depth of penetration or the volume of fluid or gas passing through a sample. Wall shear stress (WSS), on the other hand, is the force that induces material deformation through slippage along parallel planes under applied stress. Various studies have explored factors influencing permeability and WSS. For instance, Lesman et al. utilized CFD simulations to examine cellular growth within scaffold channels during perfusion cell culturing [6]. Another study investigated the impact of porosity and pore size on permeability through experimental and computational analyses [7], revealing that higher porosity and larger pore size enhanced permeability while reducing WSS. The reported average WSS typically ranges from 0.1 to 10 mPa, while cancellous bone permeability falls within 10^{-8} to 10^{-7} [3]. In this study, honeycomb-structured scaffolds with varying pore sizes were designed and analyzed using computational fluid dynamics (CFD) to assess permeability and WSS.

2.1 METHODOLOGY

This section discusses the progression of the project from initiation to completion. This research begins with a study on bone tissue engineering using a honeycomb structure. The honeycomb structure is first created using 3D SOLIDWORKS software, followed by computational fluid dynamics (CFD) simulation of blood flow within the honeycomb structure using ANSYS software. The first step involves designing the ideal honeycomb structure and analyzing the results using ANSYS Fluent. The results are then compared with previous studies to establish a benchmark. Next, different honeycomb structures are designed with varying porosity sizes. These results are subsequently compared with the ideal honeycomb scaffold geometry. The objective of this methodology is to evaluate key parameters such as velocity, wall shear stress, and pressure drop

2.1.1 GEOMETRY

To create visually appealing compositions, geometric patterns and shapes can be created and altered in art and design. A few tools and techniques that can be utilized for this are pencil and paper, CAD software, and manual techniques like sculpting and 3D printing. However, gathering data and reviewing prior research that is relevant to a research issue should come before developing a 3D design. When examining prior research, the following topics are prioritized: wall shear stress, permeability, and bone scaffold geometry.

2.1.2 HONEYCOMB DESIGN

Originating from the honeycomb seen in nature, honeycomb structures are made up of parallel stacks in the out-of-plane direction and uniformly distributed multiple-layered unit cells along the in-plane direction. Because honeycombs are more porous and less dense than the matrix materials they are made of, they have a high specific stiffness, strength, and energy absorption capacity. A wide range of engineering fields, including aerospace, architecture, automotives, semiconductors, railroad vehicles, electronic communication, nanofabrication, and medical implants, have developed and utilized honeycomb structures due to their advantageous physical properties, which include light weight, impact resistance, vibration and noise reduction, compression–torsion, negative Poisson's ratio, thermal expansion, etc [8].

Using SolidWorks, the process of crafting the honeycomb structure initiated by outlining a hexagonal pattern, serving as the representation of the honeycomb cell's cross- section. Illustrated in the Figure 1 was a 3D model of this hexagonal pattern, featuring an inner circle with a diameter of 3.4 mm and an outer circle with a diameter of 4.40 mm. Following this depiction, the outlined pattern underwent extrusion, a method where it was extended by 1 mm, ultimately converting it into a solid three-dimensional block.

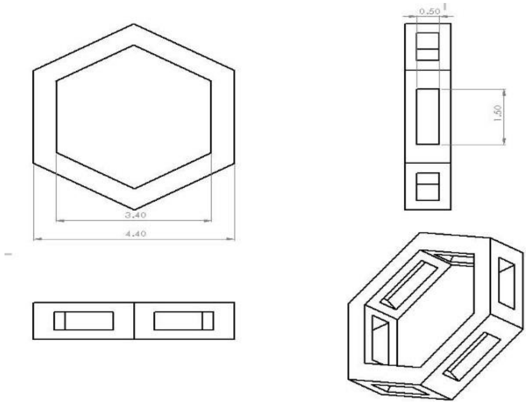

Figure 2.1 Hexagonal structure (unit in mm)

This transformation allowed the initial hexagonal sketch to evolve into a tangible and spatial object. To enhance the functionality and design, each side of the hexagon was equipped with six holes, each measuring 0.5 mm by 1.0 mm in dimensions. These intricacies in design contribute to the overall structure, reflecting both precision and attention to detail in the creation of the honeycomb configuration.

By utilizing assembly techniques, the task involves bringing together a total of 19 individual 3D hexagonal structures to construct a unified honeycomb framework. This assembly process entails aligning and connecting each of the 3D hexagonal components in a strategic arrangement in Figure 2.2 and Figure 2.3, ensuring that they seamlessly integrate to form the desired honeycomb structure. The purpose of this assembly is to combine the individual hexagonal elements into a cohesive and functional whole, reflecting the characteristic geometry of a honeycomb.

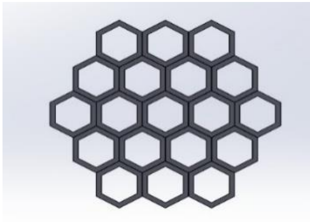

Figure 2.2 Base honeycomb structure

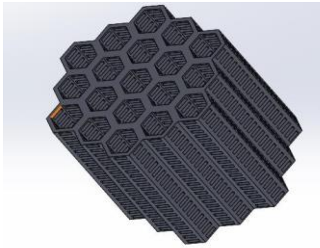

Figure 2.3 Complete 3D honeycomb structure

Upon finalizing the individual bases of the honeycomb structure, the next step involves consolidating all 40 of these bases to form the completed design. In the software SolidWorks, the "combine" feature is employed to unite all the distinct parts of the honeycomb structure into a single, cohesive entity show in Figure 3. This process entails utilizing the combining functionalities provided by SolidWorks to merge, connect, or assemble the individual components seamlessly. By executing the "combine" operation, the various parts are integrated to create a unified and comprehensive honeycomb structure, ensuring that all elements work together harmoniously to achieve the desired design outcome. In Figure 2.4, The height of honeycomb scaffold is 20 mm and the diameter is 20.32 mm.

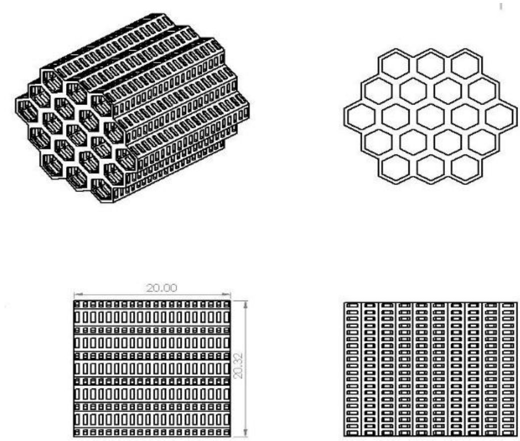

Figure 2.4 Drawing 3D honeycomb structure (Unit in mm)

2.1.3 CFD SIMULATION OF HONEYCOMB STRUCTURE

In this study, the simulation tool of choice is Ansys Fluent, dedicated CFD analyses software. The objective is to conduct simulations on CFD models of a honeycomb structure with the intention of applying the findings to human bone scenarios. The primary goal of this methodology is to ascertain key parameters, specifically the values of wall shear stress and velocity within the honeycomb structure. The simulation process encompasses several integral steps. Initial pre-processing involves preparing the 3D geometry of the honeycomb structure for analysis. Subsequent meshing is crucial for effective simulations, dividing the structure into elements for precise fluid flow analysis. Boundary conditions are then defined to simulate real-world interactions accurately. Fluid properties, such as viscosity and density, are specified to ensure the simulation mirrors reality. Finally, utilizing Ansys Fluent's advanced solver, the simulation runs, solving the governing fluid dynamics equations and providing insights into the wall shear stress and velocity characteristics of the honeycomb structure. This holistic approach covers pre-processing, meshing, boundary conditions, fluid properties, and the Fluent solver steps, collectively contributing to a comprehensive CFD simulation of the honeycomb structure.

2.1.4 ENCLOSURE

In the context of ANSYS simulation for a honeycomb scaffold, the enclosure serves as a critical component to define the boundaries and conditions for the CFD analysis. The enclosure encapsulates the honeycomb structure, providing a computational domain within which fluid dynamics simulated. The definition of the enclosure involves specifying the outer boundaries and any inlet and outlet surfaces for the fluid flow. This process is crucial for accurately capturing the interactions between the fluid and the honeycomb scaffold. Precise geometry representation and appropriate boundary conditions within the enclosure are essential for obtaining reliable results. Additionally, the enclosure setup involves specifying environmental factors, material properties, and any relevant constraints that impact the simulation. A well-defined enclosure ensures that the CFD analysis within ANSYS captures the intricate fluid behavior around the honeycomb scaffold, providing insights into parameters such as wall shear stress and velocity critical for understanding its performance in practical applications.

The enclosure was implemented are follows; First, use the Design Modeler (DM) module to check and modify the geometry if necessary, ensuring it is suitable for CFD analysis. Then, define the computational domain by constructing an enclosure around the honeycomb scaffold (Figure 5). Generate a cylinder that encompasses the entire structure. Figure 3-7 shows all the command in the DM. Specify the surfaces that will act as inlet and outlet boundaries for fluid flow within the enclosure. These surfaces are crucial for setting up boundary conditions.

2.1.5 MESHING

Meshing in CFD involves dividing a complex geometry into smaller, simpler parts called elements or cells. This process creates a mesh, which is a grid that helps simulate the fluid flow within the geometry. The quality and size of the mesh elements significantly affect the accuracy and efficiency of the simulation. The focus during the mesh generation was on the type of geometry meshed, and for the simplicity of implementation, the study employed tetrahedra as the chosen geometric type and quadratic element order. The mesh statistics reveal a total of 3102926 nodes and 2118367 elements, consistently using the tetrahedral meshing method throughout the model. Figure 2.5 shows meshing with element size of 0.27 mm and the close-up image revealing the detailed and regular pattern of these mesh elements. Using a 0.27 mm element size allows for high accuracy in the analysis, capturing fine details of model for honeycomb scaffold.

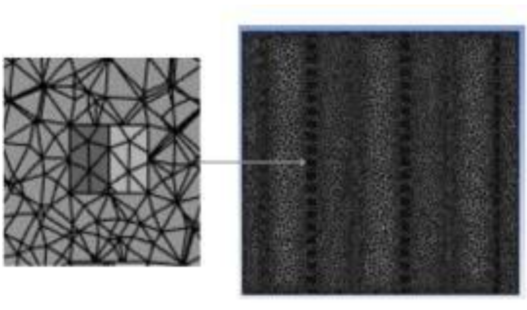

Figure 2.5 Meshing of honeycomb scaffold

2.1.6 BOUNDARY CONDITION

The simulation input for the honeycomb scaffold in this study is important for carrying out the CFD analysis. The parameter for the boundary condition can be set up to run the solver based on the zone type of model. Figure 6 shows the model with specified boundaries: the inlet where fluid enters, the outlet where fluids exits and the wall cylinder which acts as a solid boundary around the honeycomb scaffold.I n CFD simulations, setting boundary conditions is crucial for defining fluid interactions. The inlet boundary condition specifies fluid properties such as velocity and pressure as it enters the scaffold. The outlet condition defines how the fluid exits, setting pressure. The wall cylinder uses a no-slip condition, meaning the fluid velocity at the wall is zero and fluid cannot penetrate or slip along this surface.

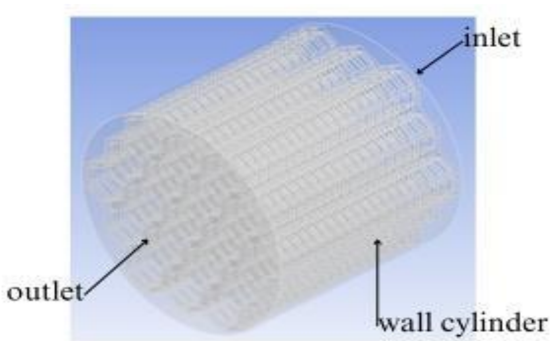

Fig. 2.6 Boundary condition of honeycomb scaffold

2.1.7 MATHEMATICAL FORMULATION

Blood flow is governed by the incompressible Navier-Stokes equation. A drop-in fluid velocity in that region indicates the impact of an expanding thrombus on blood flow. The major equation of motion used to evaluate the blood flow in the fluid domain in three dimensions is the Navier-Stroke equation. The concept of incompressible continuity states that mass entering a system equals mass leaving it. The Navier-Stokes equation is displayed as follows:

Continuity equation,

$$\nabla \cdot \mathbf{v} = 0 \tag{1}$$

Navier-Stokes equation,

$$\rho\left(\frac{\partial u}{\partial t} + u\frac{\partial u}{\partial x} + v\frac{\partial u}{\partial y} + w\frac{\partial u}{\partial z}\right) = -\frac{\partial p}{\partial x} + \mu\left(\frac{\partial^2 u}{\partial x^2} + \frac{\partial^2 u}{\partial y^2} + \frac{\partial^2 u}{\partial z^2}\right) + f_x \tag{2}$$

$$\rho\left(\frac{\partial v}{\partial t} + u\frac{\partial v}{\partial x} + v\frac{\partial v}{\partial y} + w\frac{\partial v}{\partial z}\right) = -\frac{\partial p}{\partial y} + \mu\left(\frac{\partial^2 v}{\partial x^2} + \frac{\partial^2 v}{\partial y^2} + \frac{\partial^2 v}{\partial z^2}\right) + f_y \tag{3}$$

$$\rho\left(\frac{\partial w}{\partial t} + u\frac{\partial w}{\partial x} + v\frac{\partial w}{\partial y} + w\frac{\partial w}{\partial z}\right) = -\frac{\partial p}{\partial z} + \mu\left(\frac{\partial^2 w}{\partial x^2} + \frac{\partial^2 w}{\partial y^2} + \frac{\partial^2 w}{\partial z^2}\right) + f_z \tag{4}$$

where u is the fluid flow velocity in m/s, μ is the fluid dynamic viscosity, ∇ indicates the del operator, p is the pressure in *Pascal*, and f represents additional forces like centrifugal or gravitational force. ρ marks the fluid density. f is regarded as zero in this instance [4].

Inertia forces make up one side of the Navier-Stokes equations, which explain fluid dynamics, while pressure, body, and viscous forces make up the other. The fluid's dynamic viscosity in the i-direction is used to represent the body force, and *u*, *v*, and *w* stand for the fluid's velocities in the *x*, *y*, and *z* directions, respectively.

Newton's law of viscosity determined the wall shear stress (τ_w) that the Newtonian fluid applied to the entire scaffold surface. It can be found as:

$$\tau_w = \mu \frac{\partial u}{\partial n} \tag{5}$$

where, *u* is the fluid flow velocity in *m/s*, *n* indicates *x*, *y*, and *z* directions. The permeability (*K*) of the scaffolds was evaluated using Darcy's law as follows

$$\kappa = v_D \times \mu \times \left(\frac{L}{\Delta P_{i-o}}\right) \tag{6}$$

where, v_D is the Darcy's velocity in *m/s*, *L* is the model length in *meters*, $\Delta p_{i\text{-}o}$ represents the pressure drop across inlet and outlet in *Pascal.*

2.1.8 NUMERICAL SETUP

The fluid computational domain was established by executing a boolean subtraction of the 3D scaffold design from a fluid cubical bioreactor with dimensions of 25 × 25 × 25 mm^3 for validation purposes, and from a fluid cylindrical bioreactor with a radius of

0.0002 m and plane-z alignment to investigate the impact of varying pore sizes and velocities on permeability and wall shear stress. The bioreactor's dimensions were deliberately maintained larger than the scaffold to facilitate the analysis of fluid flow through the porous scaffold in the absence of applied force. This fluid domain was subsequently exported in IGES format. In the pre-processing phase of the CFD simulation, the fluid domain bioreactor was discretized using a tetrahedral mesh. A mesh element size of 0.5 mm was employed for validation, whereas a finer mesh element size of 0.27 mm was utilized to study the effects of different pore sizes and velocities on permeability and wall shear stress. Additionally, a quadratic element order was implemented to ensure precise and accurate results.

The CFD simulation of the scaffold was performed using ANSYS Fluent 19.2, utilizing the Navier–Stokes viscous-laminar model. To simulate the properties of a cell culture environment, Dulbecco’s Modified Eagle Medium (DMEM) was selected as the working fluid, characterized by a viscosity of 0.00145 Pa·s and a density of 1000 kg/m^3. The fluid was treated as homogeneous and incompressible, with scaffold deformation due to fluid interaction being disregarded. A uniform inlet velocity of 0.001 m/s was applied along the Z-axis in the upward direction through the scaffold, while the outlet was maintained at zero pressure. No-slip boundary conditions were enforced on the walls. The simulation employed a steady-state, pressure-based absolute solver and was iterated 10,000 times to ensure convergence. Following the completion of the CFD analysis, the influence of varying velocity on permeability and wall shear stress (WSS) was examined, and the results were subsequently analyzed.

2.1.9 VALIDATION

PLA-based nature-inspired architecture for bone scaffolds: A finite element analysis reported by [3] was selected as the validation process. The velocity inlet in this study is 0.001 m/s. The blood density is 1000 kg/m^3 while viscosity is 0.00145 Pa-s and as usual the value of outlet pressure defines as zero. The geometry of the honeycomb bone scaffold, as illustrated in the Fig 7, serves as the basis for this study. In this current investigation, an identical honeycomb bone scaffold geometry was reproduced for comparative analysis. Another parameter of the scaffold was shown in Table 2.1.

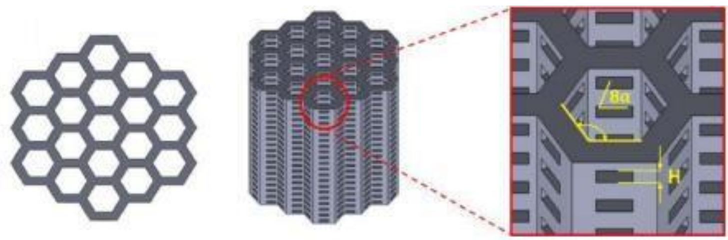

Fig. 2.7 Honeycomb bone scaffold

Table 2.1 Parameter of honeycomb bone scaffold

Pore thickness *H* (*μm*)	Pattern Angle *α* (degree)	Number of layers
500	15	40

2.1.10 DIFFERENT POROSITY ON HONEYCOMB SCAFFOLD

To analyze the behavior of scaffolds under static wall shear stress (WSS), fluid velocity, and static pressure, 3D CAD models of five porous scaffolds with nature-inspired architectures were created using SolidWorks. Each scaffold was designed with a diameter of 20.32 mm and a height of 20 mm. The design concepts based on these patterns are illustrated in Figures 8 to Figure 12. For each scaffold, certain design parameters remain consistent, including an outer hexagonal structure with a diameter of 4.4 mm and 40 repeating unit layers. However, other parameters, such as porosity size, vary depending on the scaffold's geometry. The overall height of each scaffold is maintained at a fixed 20 mm.

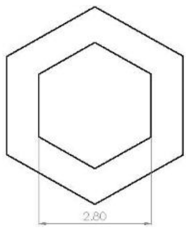

Fig. 2.8 Hexagonal structure with 2.8 mm porosity

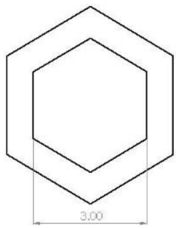

Fig. 2.9 Hexagonal structure with 3.0 mm porosity

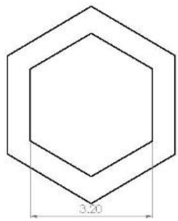

Fig. 2.10 Hexagonal structure with 3.2 mm porosity

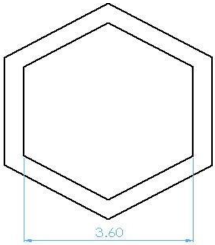

Fig. 2.11 Hexagonal structure with 3.6 mm porosity

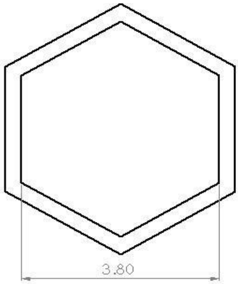

Fig. 2.12 Hexagonal structure with 3.8 mm porosity

The porosity of all CAD models above 70%, determined by evaluating the designed volume of each scaffold in SolidWorks. The designed porosity (PCAD) is computed using Equation 6 shown in Table 2, where VBulk represents total volume of the CAD, and VCAD is the designed volume of the scaffold.

$$PCAD = \left(1 - \frac{VCAD}{VBulk}\right) \times 100\% \quad (7)$$

Table 2.2 Table of porosity of all scaffolds

Pore size (mm)	2.8	3.0	3.2	3.4	3.6	3.8
Porosity (%)	70.25	72.83	75.75	78.98	82.54	86.42

2.2 RESULT AND DISCUSSION

In Figure 13 shows WSS contours for different porosity sizes in a hexagonal structure. Smaller porosities (2.8mm and 3.0mm) have higher and more concentrated shear stress, shown by red and yellow areas. Larger porosities (3.6mm and 3.8mm) have lower and more evenly distributed shear stress, shown by blue and green areas. This means larger porosities reduce stress concentrations and improve structural integrity. The analysis of WSS and permeability reveals notable trends as the pore size varies. Permeability were calculated with Darcy's Law using Equation 8 as shown in Table 3. The highest wall shear stress is observed at a pore size of 3.0 mm, with a value of 3.99 mPa, while the lowest wall shear stress occurs at a pore size of 3.6 mm, measuring 2.91 mPa. In terms of permeability, the highest value is found at a pore size of 3.8 mm, with $2.468\times10{-7}$, whereas the lowest permeability is at a pore size of 2.8 mm, with $6.362\times10{-8}$. The best pore size is 3.8 mm because has the highest value of permeability and second lowest of WSS.

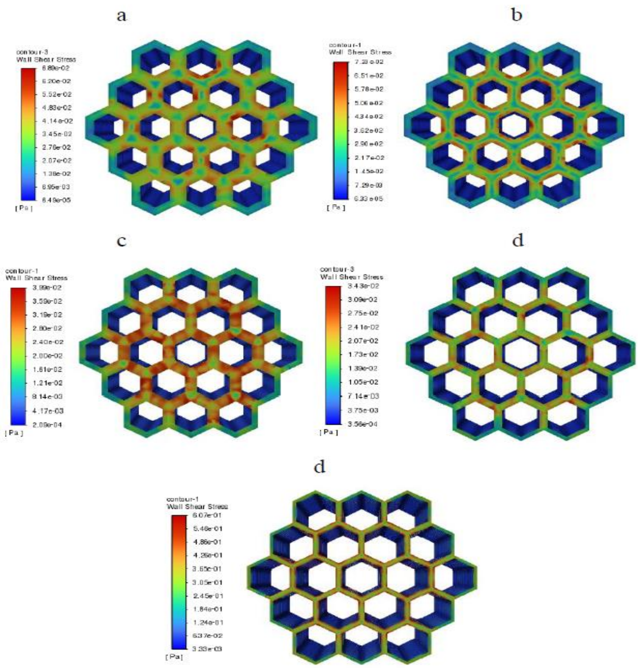

Fig. 2.13 Wall shear stress at inlet on different size of porosity a)2.8mm b)3.0mm c)3.2mm d)3.6mm e)3.8mm

Table 2.3 Wall shear stress and permeability on different porosity

Pore Size (mm)	Wall shear stress (mPa)	Pressure drop (Pa)	Permeability
2.8	3.83	0.4505	6.362 × 10-8
3.0	3.99	0.3389	8.457 × 10-8
3.2	3.87	0.2623	1.093 × 10-7

3.6	2.91	0.1518	1.889 × 10-7
3.8	3.01	0.1161	2.468 × 10-7

2.3 CONCLUSION

This study provides valuable insights into the fluid dynamics within honeycomb scaffolds, with a particular focus on the correlation between pore size, permeability, and wall shear stress (WSS). Across all scaffolds, the permeability ranged from 6.362×10^{-8} to 2.468×10^{-7}, which falls within the required range for cancellous bone (10^{-8} - 10^{-7}). The CFD results for WSS were found to be within 2.91 – 3.99 mPa, meeting the requirements for cell differentiation (2.91 – 3.99 mPa). The findings indicate that larger pore diameters enhance permeability, allowing for smoother fluid flow through the material. However, the relationship between WSS and pore size is not linear. Initially, WSS increases as pore size increases, up to a certain point, after which it begins to decrease as pore size continues to grow. This pattern suggests that smaller pores intensify fluid-wall interactions, resulting in higher WSS. Conversely, larger pores reduce these interactions, leading to a decrease in WSS. These findings highlight the importance of optimizing pore size to achieve the ideal balance between permeability and WSS, ensuring the effective performance of scaffolds in biomedical applications

BIBLIOGRAPHY

[1] H. Montazerian, E. Davoodi, M. Asadi-Eydivand, J. Kadkhodapour, and M. Solati-Hashjin, “Porous scaffold internal architecture design based on minimal surfaces: A compromise between permeability and elastic properties,” Mater. Des., vol. 126, pp. 98–114, Jul. 2017.

[2] M. Kamel, M. Ahmed, and A. Sethi, “Regional anesthesia for orthopedic procedures: What orthopedic surgeons need to know,” World J. Orthop., vol. 13, no. 1, pp. 11–35, 2022.
[3] S. S. Mohol, M. Kumar, and V. Sharma, “PLA-based nature-inspired architecture for bone scaffolds: A finite element analysis,” Comput. Biol. Med., vol. 163, Art. no. 107163, Sep. 2023.
[4] D. Ali and S. Sen, “Permeability and fluid flow-induced wall shear stress of bone tissue scaffolds: Computational fluid dynamic analysis using Newtonian and non-Newtonian blood flow models,” Comput. Biol. Med., vol. 99, pp. 201–208, Aug. 2018.
[5] Y. Li et al., “The effect of mechanical loads on the degradation of aliphatic biodegradable polyesters,” Reproduction, vol. 153, no. 6, pp. R207–R219, Jun. 2017.
[6] A. Lesman, Y. Blinder, and S. Levenberg, “Modeling of flow-induced shear stress applied on 3D cellular scaffolds: Implications for vascular tissue engineering,” Biotechnol. Bioeng., vol. 105, no. 3, pp. 645–654, Feb. 2010.
[7] M. R. Dias, P. R. Fernandes, J. M. Guedes, and S. J. Hollister, “Permeability analysis of scaffolds for bone tissue engineering,” J. Biomech., vol. 45, no. 6, pp. 938–944, Apr. 2012.

[8] Q. Zhang et al., “Bioinspired engineering of honeycomb structure—Using nature to inspire human innovation,” Prog. Mater. Sci., vol. 74, pp. 332–400, 201